

Observations of Circinus X-1 with RXTE

Hale Bradt ^a, Robert Shirey & Alan Levine

^aCenter for Space Research and Department of Physics
Massachusetts Institute of Technology
Room 37-587
Cambridge MA 02178 USA

Data accumulated with RXTE during the active state of Cir X-1 as well as during an unusually long transition from the active state to the quiescent state are reported. The long decline from the active state allowed the source characteristics to be studied systematically as a function of intensity. The following results are presented: (1) spectral fits during entry into a dip clearly show absorption with partial covering as previously reported (Brandt et al. 1996), and (2) correlations between position in the hardness-intensity plane and the character of the power density spectrum as the source entered the quiescent state are suggestive of Z source behavior seen in LMXB sources.

1. INTRODUCTION

Circinus X-1 is a highly variable X-ray source that exhibits periodic activity every 16.6 d which is widely attributed to an eccentric binary orbit with the activity occurring at periastron in X-rays, infrared/optical, and radio (Kaluzienski et al. 1976; Glass 1978; Whelan et al. 1977; Moneti 1992). The detection of bursts with EXOSAT, almost surely of type I, indicates the source is very likely a low-mass binary (Tennant, Fabian & Shafer 1986); see also Glass (1994). It has also been suggested that the binary was ejected from a nearby supernova (which formed the neutron star) and is thereby very young (30 000 to 100 000 y; Stewart et al. 1993). A young age would be in accord with the eccentric orbit. Also, quasi-periodic oscillations (QPO) have been reported in EXOSAT data by Tennant et al (1987, 1988) and others (see Oosterbroek et al. 1995) at 1.4 Hz, 5–20 Hz and 100–200 Hz.

More recently, a study with ASCA of a transition from a low state of Cir X-1 to a high state showed it to be caused by absorption with partial covering (Brandt et al. 1996). RXTE observations of the quiescent phase of one 16-d cycle showed strong correlations in RXTE data between various features in the PDS including a quasi periodic oscillation that moved from 1.3–

12 Hz during the quiescent part of the cycle (Shirey et al. 1996). A reanalysis of EXOSAT observations led Oosterbroek et al. to propose that the neutron star has a very low magnetic field with, on occasion, an accretion rate that reaches the Eddington level; see also van der Klis (1994).

Here we present new RXTE results on the nature of the 16.6-d cycles, the absorption in dips, and the QPO in the quiescent and active phases. The work presented briefly here will be presented more fully in a forthcoming publication by Shirey and colleagues.

2. RESULTS

2.1. Long-term behavior - ASM

The record of Cir X-1 from the All-Sky Monitor (1.5–12 keV) of RXTE shows it to have been remarkably consistent in its behavior over the past 20 months. A sample ASM light curve covering five of the 16.5-d cycles is shown in Fig. 1. The quiescent phases have remained at about 1.0 Crab. This is unusual in the context of past epochs when Cir X-1 has been below thresholds of detection or weaker and less active. In other words, it exhibits significant long-term (years) variability (e.g. Oosterbroek et al.). In the ASM data, the active phases show increased fluxes, a generally softer spectrum, and chaotic behavior

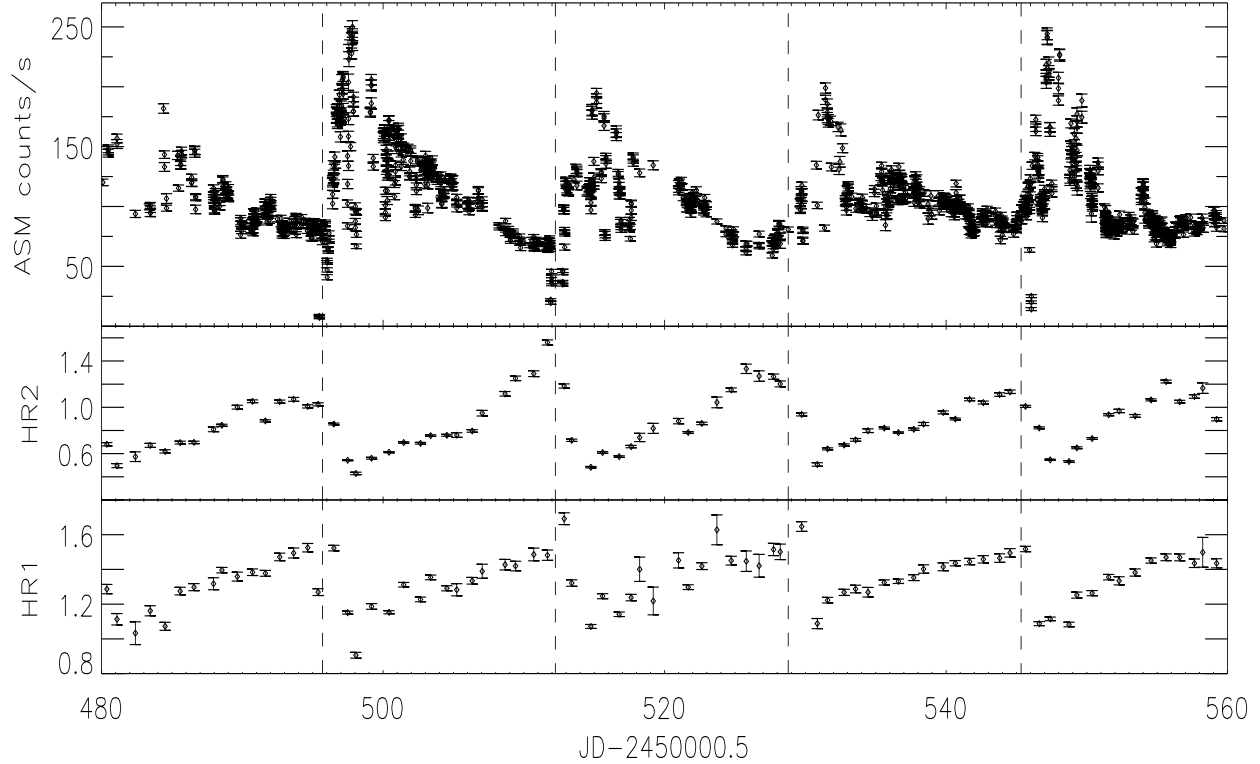


Figure 1. ASM light curve (1.5–12 keV) and hardness ratios for 80 days. HR1 is 3–5/1.5–3 and HR2 is 5–12/3–5, all in keV. Dashed lines are zero-phase markers (Stewart et al. 1991). Eight PCA observations were carried out during the 16-d cycle (1997 Feb. 16 - Mar. 6, or at Day \sim 500) which exhibits the slow descent.

(Fig. 1). These features were generally known before but not in such a comprehensive context. The figure also shows the general hardening of the spectrum during the quiescent phases previously reported (Shirey et al.) and earlier observed in folded data with the Ginga ASM data (Tsunemi et al. 1989).

The duration and level of activity during the active states can vary significantly from one cycle to another (Fig. 1). In particular we note the active state occurring at day 500 in Fig. 1. It was unusually slow in its descent to the quiescent phase. Such a slow descent allows one to study the spectral and temporal behavior as a function of luminosity and/or state.

2.2. High-statistics PCA Observations

A major study of Cir X-1 with the RXTE PCA has been undertaken by the present authors. The source has been studied during several active phases with high (about 60 percent) coverage and for several complete 16-d cycles, typically with sampling every two days. To date the observing time amounts to 840 ks. These data, soon becoming public, exhibit Cir X-1 undergoing a wide variety of spectral/temporal states.

PCA observations taken on 1996 Sept. 21 exhibited a dramatic dip which is presented herein. (There are others in the archive.) Also, eight observations at 2-day intervals were obtained (fortuitously) during the 1997 Feb-Mar cycle wherein there was a slow descent from the active state as noted above. The results from these latter observations are presented here also. Each of these eight observations lasted for 6 ks; they are designated Obs. I - VIII in time order.

2.3. Dips

Low states or dips are seen in Fig. 1 to occur very close to phase zero. They systematically precede the subsequent increase of flux and flaring behavior of the active state. They should be an important indicator of the geometry of the matter in the binary system.

The dips are beautifully elucidated in the PCA data with sufficient statistics to follow the spectra during the transition into the dip. One such dip on 1996 Sept. 21 is shown in Fig. 2 with a

hardness ratio. Note the hardening during entry and the softness during the minimum.

The six times marked in Fig. 2 were chosen for the determination of energy spectra, one before entry into the dip, four during the descent, and one in the dip at low flux. They are numbered sequentially from 1 to 6. (Do not confuse with the observation numbers I - VIII used for the 1997 data.) The six count-rate spectra are shown in Fig. 3, together with fits through the data points. The spectrum taken at time 1 is uppermost. The underlying continuum model is a disk-blackbody plus a power law with absorption of $2 \times 10^{22} \text{ cm}^{-2}$ (Predahl and Schmitt 1995; Brandt et al.). This (interstellar) absorption was held fixed for the fits. The PL and DBB components were allowed to vary but were constrained to be the same for all six spectra. In addition, the model included partial covering. The parameters for this were allowed to vary, namely the column density and fraction covered.

The fits give do not give satisfactory chi square values because of the imposed constraints, but they do provide qualitative insight into the transition. The partial covering is evident in that the flux in the lowest channel reaches a minimum in spectrum 4 and is approximately constant thereafter. The absorption has become so great that, in the covered region, the low-energy flux is completely absorbed, and only the uncovered flux remains. Thereafter the absorption affects only higher and higher energies, with iron absorption being pronounced as one can see from the structure in the lower two spectra, #5 and #6.

The covering fraction was set to zero for spectrum #1. The fits for spectra #2 to #6 yield values increasing monotonically from 0.45 to 0.87. The major differences in the spectra are the column densities of the partial covering. They too show a monotonic increase from zero for spectrum #1 and then from 17 ± 1.5 up to 675 ± 102 for observations #2 to #6, in units of 10^{22} cm^{-2} . Note that spectrum #6 has N_H exceeding 10^{24} cm^{-2} . This is in accord with the absorption found by Brandt et al.

Although this absorption was reported earlier, it is reassuring to find that this broad-band spectral approach provides similar conclusions. Also,

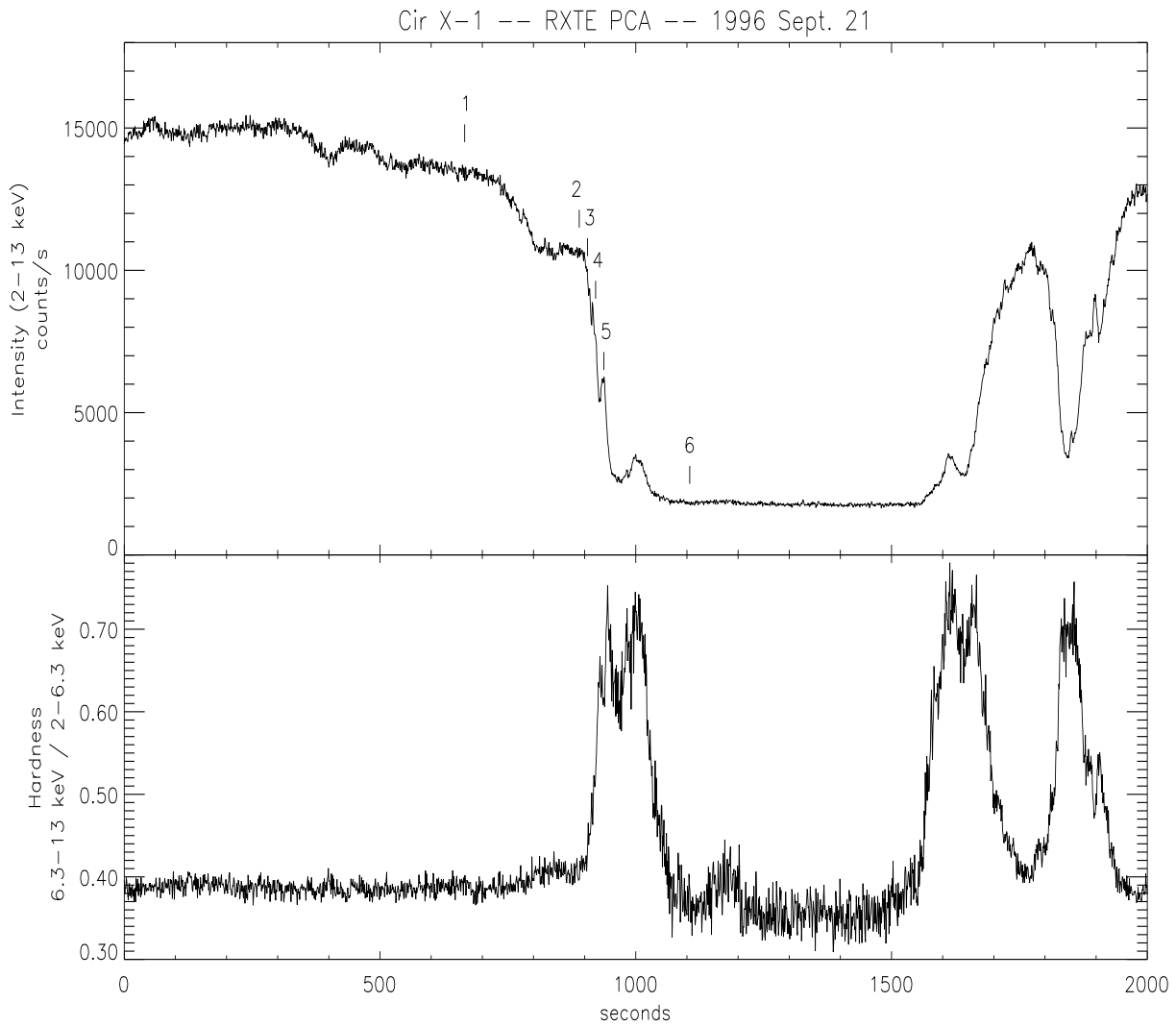


Figure 2. Dip of duration ~ 800 s in PCA data, from 1996 Sept. 21.

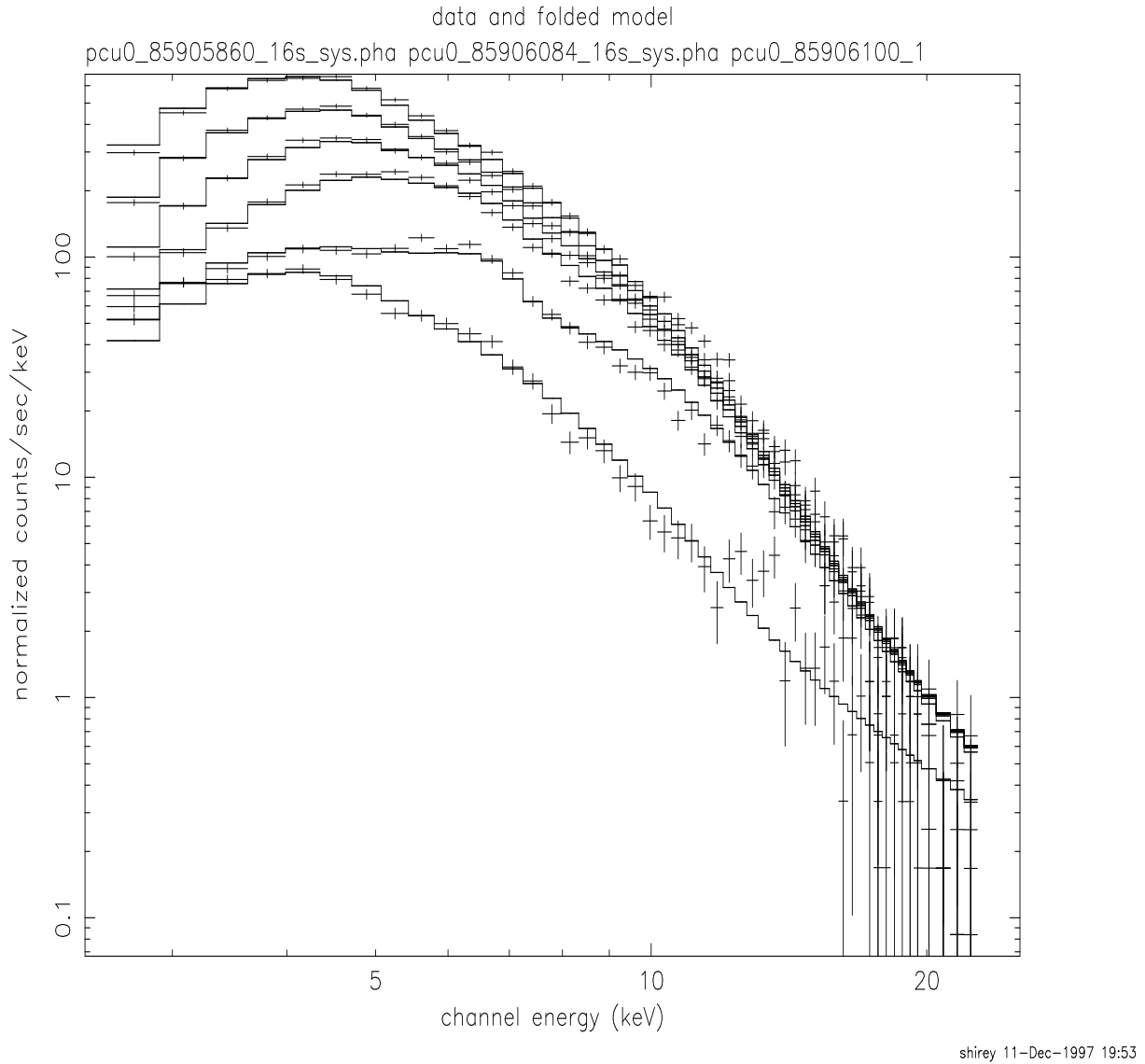


Figure 3. Data and spectral fits for the times indicated by the numerals 1 to 6 in Fig. 2. Spectrum 1 is the uppermost and spectra 2 - 6 sequentially decrease at 4 - 6 keV.

this work places the absorption clearly in the context of the well-defined dips seen in the ASM and PCA data.

2.4. Quasi-periodic oscillations

The RXTE data from the eight 6-ksec observations during the long descent of 1997 Feb. - Mar. clarify significantly the behavior of the QPO's in Cir X-1. As noted, QPO at 5–20 Hz were apparent in EXOSAT data. Oosterbroek et al. associated these with normal-branch oscillations that are associated with instabilities in the accretion flow under conditions of high luminosity (Fortner, Lamb & Miller, 1989).

During the quiescent phase, Shirey et al. reported a QPO with frequency moving systematically from 1.3 to 12 Hz as well as other features in the PDS. Additional RXTE data now show that this QPO moves all the way up to 30 Hz (Fig. 4a,b). In addition, during the active state, a strong 4-Hz oscillation can develop in concert with the fading 30-Hz oscillations (Fig. 4c) and then can become quite strong (Fig. 4d). The 4-Hz QPO can give way to strong very-low-frequency noise due to active flaring and dips (Fig. 4e) or to strong unpeaked noise (Fig. 4f), all during the active state. The 4-Hz oscillation always appears at the same frequency and is often apparent. (Recent analyses by Shirey suggest that Fig. 4f may be a variant of Fig. 4c which occurs near the HB-NB apex; see below.)

The 1–30 Hz QPO frequency increases very strongly with 2–18 keV intensity during the relatively small changes of intensity during quiescence. In contrast, the 4-Hz QPO occurs over a wide range of intensities and is quite constant. The latter QPO is reminiscent of “normal branch” oscillations in the LMXB sources exhibiting ‘Z’ behavior in the color-color (CCD) and hardness-intensity (HID) diagrams (Hasinger & van der Klis 1989). An example is the 6-Hz QPO in Sco X-1 (Middleditch & Priedhorsky 1986). This further suggests that the 1–30 Hz QPO are “horizontal-branch” QPO in the same scheme. Indeed, the frequency increases with intensity as do horizontal branch oscillations. Such oscillations are indicative of a significant magnetic field in beat-frequency models (Alpar & Shaham 1985;

Lamb et al. 1985).

2.5. Branches in the HID

Color-color diagrams (CCD) and hardness-intensity diagrams (HID) are shown in Fig. 5 for the same long descent from the active state in 1997 Feb. - Mar. The left two panels show all 8 observations, numbered in time sequential order from 1 to 8, while the right two are blowups of Observations V and VI which occurred just as the source was making the transition from the active to quiescent state at the end of the long descending ramp seen in Fig. 1. Each point represents 16 s of data. The scatter plot for each of the eight PCA observations tends to be isolated from that of the adjacent observation because of the large intensity and color changes.

The HID (lower panels) serve to isolate trends better than the CCD (upper panels), so our discussion here will focus on them. One immediately notes the long tails due to dipping and flaring in the earlier observations (I - IV, lower right of lower-left panel), and the lack of flaring in the last two observations (VII - VIII, upper left of same panel). The intermediate observations (V and VI) show interesting branch structure; see lower right panel.

The shape of these two observations taken together is reminiscent of Z sources. The data in this scatter plot were divided into 11 separate zones and FFT were taken for each of them. Several of the resultant PDS are shown in Fig. 4; they will be referenced in the following discussion.

Focus now on the lower right panel of Fig. 5 (HID for Obs. V and VI). The variable QPO is seen at its highest frequency (30-Hz; Fig. 4b) at the upper left end of the upper cluster (Obs. VI). Further to the right along this “horizontal branch”, the 30-Hz is fading as the 4-Hz QPO begins to appear (Fig. 4c). The 4 Hz QPO remains strong around the bend and onto the short descending “normal” branch without evidence of the 30 Hz (Fig. 4d). In the lower cluster (Obs. V), the 4 Hz QPO is present along the (longer) lower branch (continuation of the “normal” branch?). Only large low frequency power is found on the upper (“flaring”?) branch of this observation (Fig. 4e).

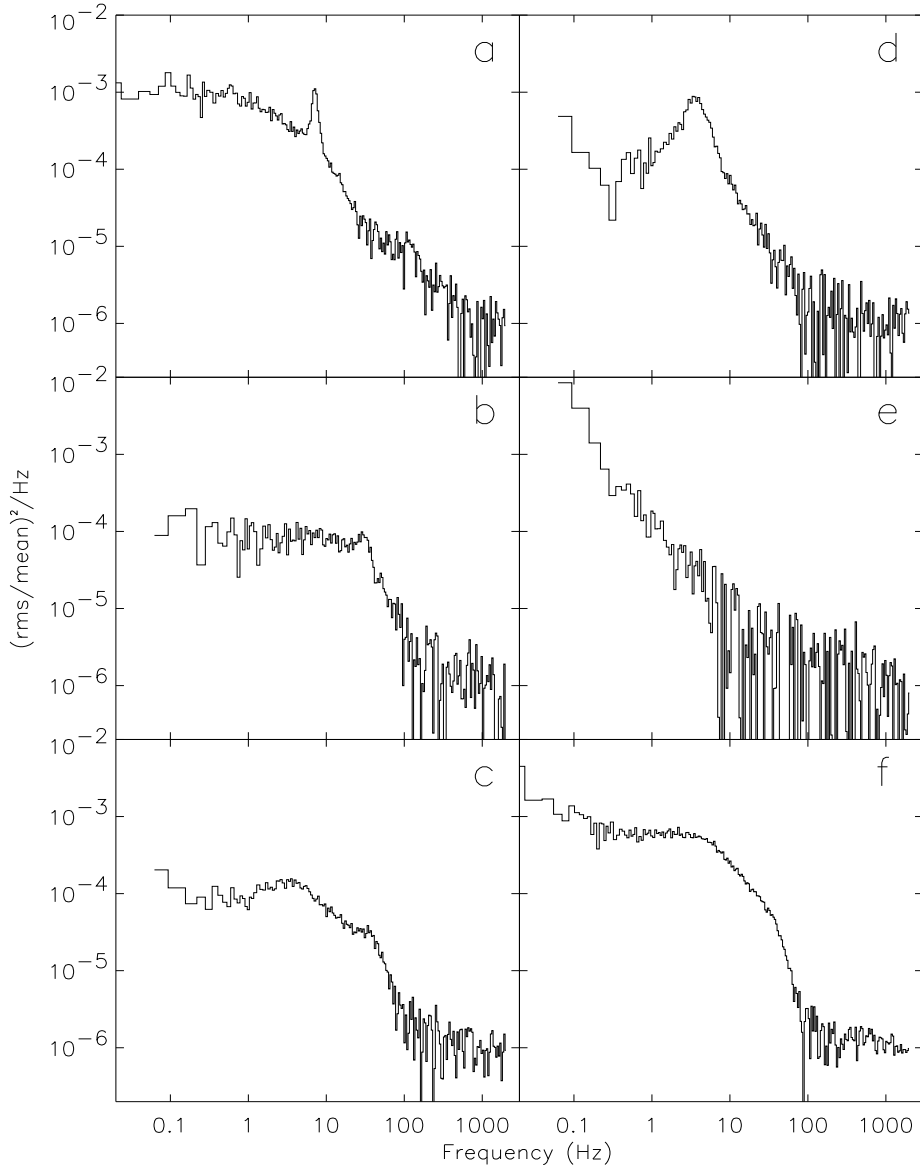


Figure 4. Power density spectra for six 1000-s intervals in the 1997 Feb.-Mar cycle of Cir X-1, shown in order of postulated increase in accretion rate (i.e., more or less time reversed): (a) the variable 1-12 Hz QPO seen at 7-Hz during quiescence in Obs. VIII, (b) the same QPO in Obs. VI where it is found at 30-Hz, (c) The constant 4-Hz QPO with a weakened 30 Hz ‘later’ in Obs. VI. (d) strong 4-Hz in Obs. V, (e) VLFN ‘later’ in Obs. V, (f) strong unpeaked noise in Obs. I. The latter may be a variant of (c); see note in text.

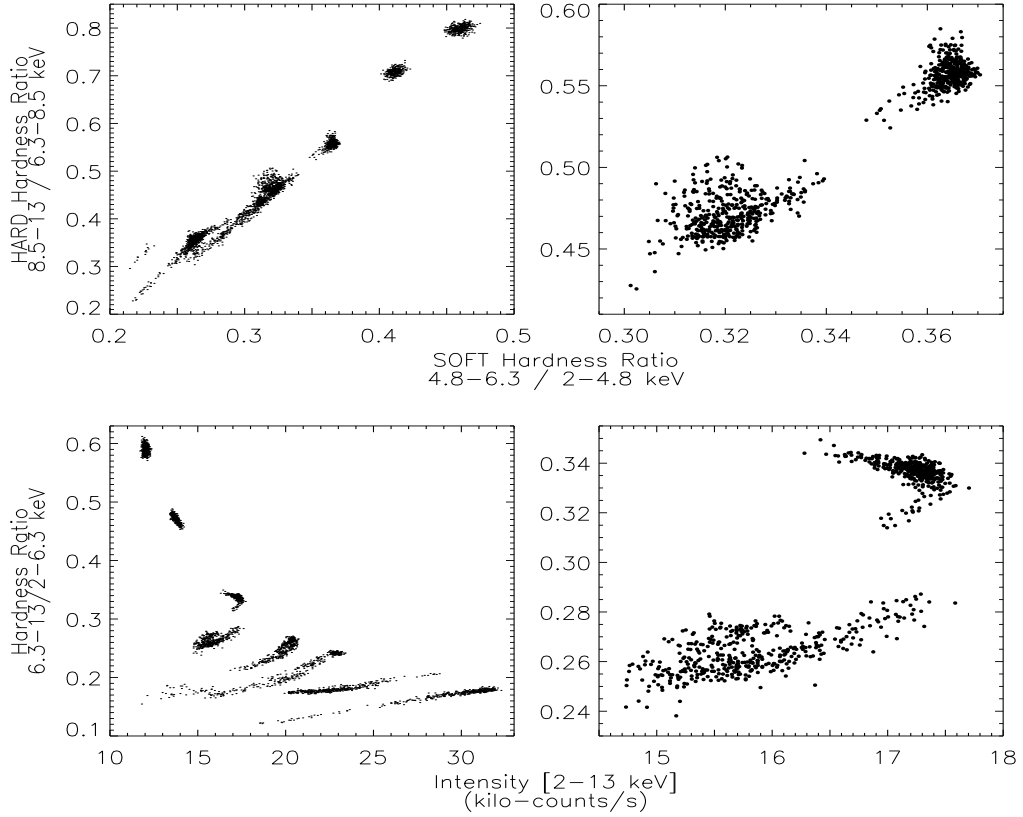


Figure 5. Left panels: all 8 observations of the 1997 Feb-Mar cycle shown in a CCD (upper panel) and in an HID (lower panel). In time order the observations (numbered I - VIII) progress from lower left to upper right in the CCD and from lower right to upper left in the HID. Right panels: expanded views of Obs. V and VI in CCD and HID. The expanded HID (lower right panel) bears similarities to the appearance of Z sources, particularly when the QPO characteristics are taken into account.

This correlation of HID branches with QPO type reinforces the association with Z sources. The postulated horizontal-branch QPO does indeed occur on a horizontal branch in the HID, and the postulated normal-branch QPO does occur on a descending branch as in Z sources. The expected variation of the 1–30 Hz QPO is not seen in the horizontal branch of Obs. VI, but this QPO appears at lower frequency at lower accretion rates, e.g. 7 Hz in Obs. VIII (Fig. 4a).

Since this talk was given, Shirey has found that a similar diagram, but with the hard color (13–18 keV/9–13 keV) on the ordinate (instead of the soft color shown here), the upper tail of the lower diagram turns downward rather than upward. Thus the perceived sequence from top to bottom (say, as \dot{M} increases) makes contiguous the 4-Hz regions, and places the “flaring” region with no QPO and strong low-frequency noise below (‘after’) the 4-Hz branch. This makes the Z-source association even stronger. There do remain differences between these diagrams and classic Z-source behavior, e.g., no Z shape in the CCD). These differences may well be related to the extreme degree of variability in this source.

3. CONCLUSIONS

The behavior of intensity, colors, and QPO during a long decrease in intensity has shown behavior clearly reminiscent of low-mass Z sources. The presence of horizontal-branch oscillations in the beat-frequency model (Alpar & Shaham; Lamb et al.) indicates a significant magnetic field. Clearly, the suggested low-magnetic-field description of the neutron star in this system (Oosterbroek et al.) should be reexamined.

The timing and nature of absorption dips has been elucidated. The pronounced dips typically occur just as the source is entering its active state, but before it has increased in intensity. These particular dips have been shown in PCA data to be absorption events with partial covering, confirming earlier work, but placing the absorption clearly within the well-defined dips at the entry to the active phase. These dips should be useful in unraveling the geometry of this unique and interesting system.

The authors thank Drs. Edward Morgan and Saul Rappaport for helpful conversations. They are also grateful to all those on the ASM and PCA teams at MIT and GSFC, to the RXTE control and data management teams at GSFC, and to NASA.

4. REFERENCES

- Alpar, M. & Shaham, J. 1985, *Nature* 316, 239
- Brandt, W. et al. 1996, *MNRAS*, 283, 1071
- Fortner, B., Lamb, F., & Miller, G. 1989, *Nature* 342, 775
- Glass, I. 1978, *MNRAS*, 183, 335
- Glass, I. 1994, *MNRAS*, 268, 742
- Hasinger, G. & van der Klis, M. 1989, *A & A* 225, 79
- Kaluzienski et al. 1976, *ApJ*, 208, L71
- Lamb, F. et al. 1985, *Nature* 317, 681
- Middleditch, J. & Priedhorsky, W. 1986, *ApJ* 306, 230
- Moneti, A. 1992, *A&A*, 260, L7
- Oosterbroek, T. et al. 1995, *A&A*, 297, 141
- Predahl, P. & Schmitt, J. 1995, *A&A* 293, 889
- Shirey, R., et al. 1996, *ApJ*, 469, L21
- Stewart, R., et al. 1991, *MNRAS*, 253, 212
- Stewart, R. et al. 1993, *MNRAS* 261, 593
- Tennant, A., Fabian, A., & Shafer, R. 1986, *MNRAS*, 221, 27p
- Tennant, A. 1987, *MNRAS*, 226, 971
- Tennant, A. 1988, *MNRAS*, 230, 403
- Tsunemi, H. 1989, *PASJ*, 41, 391
- van der Klis, M. 1994, *ApJS*, 92, 511
- Whelan, J. 1977, *MNRAS*, 181, 259.